The effect of carbonic anhydrase on foraminiferal Mg/Ca

Siham De Goeyse[1], Chiara Lesuis[1,2], Gert-Jan Reichart[1,3] and Lennart de Nooijer[1]

[1] Ocean Sciences, NIOZ—Netherlands Institute for Sea Research, Texel, Netherlands
[2] Institute for Sanitary Engineering, Water Quality and Solid Waste Management, University of Stuttgart, Stuttgart, Germany
[3] Geosciences, Utrecht University, Utrecht, Netherlands

ABSTRACT

Marine biogenic calcium carbonate production plays a role in the exchange of CO_2 between ocean and atmosphere. The effect of increased CO_2 on calcification and on the resulting chemistry of shells and skeletons, however, is only partly understood. Foraminifera are among the main marine $CaCO_3$ producers and the controls on element partitioning and isotope fractionation is the subject of many recent investigations. The enzyme carbonic anhydrase (CA) was, for example, shown to be vital for $CaCO_3$ deposition in benthic foraminifera and indicates their ability to manipulate their intracellular inorganic carbon chemistry. Here, we tested whether CA affects the partitioning of Na, Mg and Sr in the perforate, large benthic, symbiont-bearing foraminifer *Amphistegina lessonii* by addition of the inhibitor acetazolamide (AZ). The effect of dissolved CO_2 on the effect of CA on element partitioning was also determined using a culturing setup with controlled atmospheric carbon dioxide levels (400–1,600 ppm). Results show that inhibition by AZ reduces calcification greatly and that CO_2 has a small, but positive effect on the amount of calcite formed during the incubations. Furthermore, the inhibition of CA activity has a positive effect on element partitioning, most notably Mg. This may be explained by a (n indirect) coupling of inorganic carbon uptake and inward calcium ion pumping.

Submitted 18 December 2023
Accepted 14 October 2024
Published 29 November 2024

Corresponding author
Lennart de Nooijer,
ldenooijer@nioz.nl

Academic editor
Christof Meile

Additional Information and Declarations can be found on page 16

DOI **10.7717/peerj.18458**

Subjects Aquatic and Marine Chemistry, Biogeochemistry, Biological Oceanography
Keywords Foraminifera, Geochemistry, Paleoceanography

INTRODUCTION

Calcifying foraminifera are marine protists responsible for approximately half of the open ocean calcium carbonate production (*Schiebel, 2002*). Their fossil shells are also widely used as tools for reconstructing the paleoenvironment and paleoclimate. Incorporation of minor elements in their shell is used to *e.g.*, reconstruct temperature and to trace back the composition of the seawater in which they calcified. One of the most commonly used proxies in paleoceanography, next to stable oxygen isotopes, is the Mg/Ca ratio of foraminiferal shells. The amount of Mg incorporated in the calcitic shell has been shown to primarily reflect sea water temperature (*Nürnberg, Bijma & Hemleben, 1996*; *Anand, Elderfield & Conte, 2003*), but is also influenced by so-called vital effects (*Erez, 2003*; *Bentov & Erez, 2006*; *De Nooijer et al., 2014*). Although Mg/Ca is one of the most robust temperature proxies known, foraminiferal life processes such as their metabolism and the

biology involved in biomineralization is offsetting the thermodynamic relation between Mg/Ca partitioning and temperature. Such effects are species-specific and are apparent from the variability in average Mg/Ca (*e.g.*, *Bentov & Erez, 2006*; *Sadekov et al., 2016*; *Van Dijk, De Nooijer & Reichart, 2017*), variations in Mg/Ca-temperature calibrations (*Toyofuku et al., 2011*; *Wit et al., 2012*), and offsets both in ratios and Mg/Ca-temperature sensitivities between foraminifera and inorganically precipitated calcites (*Bentov & Erez, 2006*).

Understanding foraminiferal calcification is also important because of its important role in the carbon cycle because of the continuous production of calcitic shells by planktonic species in the upper water column and subsequent downward transport. It has been estimated that up to 50% of the open ocean biogenic calcium carbon flux consists of foraminiferal shells (*Schiebel, 2002*), and a collective response in calcification to climate change may thus have an impact on sea water carbonate chemistry. Calcium carbonate precipitation in the ocean shifts the carbonate chemistry in such a way that enhanced calcium carbonate precipitation increases surface water pCO_2 (*Zeebe & Wolf-Gladrow, 2001*), whereas water column dissolution reduces pCO_2 at depth, thereby *de facto* counter acting the biological carbon pump. This balance between organic and inorganic carbon transport, which is called the rain ratio, thereby plays a major role in setting atmospheric pCO_2 under natural conditions. This implies that reduced and/or enhanced foraminiferal biomineralization as a consequence of ongoing anthropogenic CO_2 emissions and associated ocean acidification potentially could provide an important negative or positive feedback (*e.g.*, *Sarmiento et al., 2002*; *Feely et al., 2004*). Since already 25% of the anthropogenic CO_2 has been absorbed by the oceans since the industrial revolution (*e.g.*, *Sabine & Tanhua, 2010*), understanding such feedback is clearly urgent and of great importance.

Foraminiferal calcification has been studied in detail to understand so-called vital effects and also to understand the impact of changes in the sea water carbonate system on calcification. Several studies looked into the way foraminifera modify the chemistry at the site of calcification (SOC) and also outside the SOC. Foraminifera are known to strongly affect the pH, both inside (*Bentov, Brownlee & Erez, 2009*; *De Nooijer et al., 2009*) and outside the SOC (*Rink et al., 1998*; *Köhler-Rink & Kühl, 2000*, *2005*; *Glas, Langer & Keul, 2012*; *Toyofuku et al., 2017*). It has been argued that active proton pumping, visible from the pH gradient between the SOC and outside the foraminifer, is directly coupled to inward Ca^{2+} transport (*Toyofuku et al., 2017*). This would involve exchange of two protons being pumped out of the SOC in exchange for one Ca^{2+} ion entering the SOC (*Nehrke et al., 2013*; *Toyofuku et al., 2017*).

The H^+-pumping has also been suggested to cause an inward diffusion of CO_2 as a result of the steep pH gradient (~9.0 at the site of calcification, ~6.5 outside low-Mg/Ca species; *Toyofuku et al., 2017*). The high pH in the calcifying fluid may also attract CO_2 from the foraminifer's cytosol, which has been invoked to explain low calcite $\delta^{13}C$ (*Schmiedl et al., 2004*). Counterintuitively, this implies that a higher ambient pCO_2 may stimulate calcification by foraminifera as it would enhance CO_2 fluxes, explaining the positive impact of CO_2 on calcification observed in some culturing experiments

(*Haynert et al., 2014*). Other studies, however, indicated that growth was hampered by elevated CO_2 levels (*Hikami et al., 2011*). This apparent contradiction between studies may be explained by the involvement of other inorganic carbon species. Bicarbonate ions (HCO_3^-) may be taken up and converted by the enzyme carbonic anhydrase (CA), an enzyme catalyzing the reversible hydration of CO_2 to form H_2CO_3 with the direction of the reaction entirely dictated by pH (*Lindskog, 1997*). Indirectly, this may also help to convert the CO_2 to CO_3^{2-} after diffusing to the site of calcification in foraminifera (*De Goeyse et al., 2021*). Although the pH inside the SOC has been measured to be close to 9 (*De Nooijer et al., 2009*), conversion of CO_2 without CA would be the rate limiting step in calcification (see *e.g.*, *Chen, Gagnon & Adkins, 2018* for the role of CA in coral calcification). This has been highlighted in other marine calcifying organisms where carbonic anhydrase was found to be an integral part of the biomineralization pathway (*Bertucci et al., 2013*; *Medaković, 2000*; *Müller et al., 2013*; *Le Roy et al., 2014*; *Wang et al., 2017*).

Here, we investigate element pumping by foraminifera during biomineralization using acetazolamide to block the functioning of carbonic anhydrase and through varying carbonate chemistry in controlled growth experiments. We focused on the foraminiferal species *Amphistegina lessonii*, a large benthic, symbiont-bearing foraminifer that forms a calcite shell as this species has been investigated in detail for its biomineralization pathways and impact of different environmental factors (*Raja et al., 2005*; *Raja, Saraswati & Iwao, 2007*; *Segev & Erez, 2006*; *De Nooijer et al., 2017*; *Geerken et al., 2018*; *Levi, Müller & Erez, 2019*; *Dämmer et al., 2021*). We measured the minor element composition of the shells produced under contrasting conditions to elucidate calcification mechanisms, elemental pathways and carbon uptake.

MATERIALS AND METHODS

Foraminifera collection and incubation

Sediments were collected from the Indo-Pacific coral reef aquarium at Burgers' Zoo in September 2021. Adult specimens of *A. lessonii* were isolated from these sediments and were incubated in Petri dishes with filtered seawater (Whatmann, 0.3 µm pore filters) for 1 week at 18 °C with a 12 h light/dark cycle and no added food. After this week they were fed living *Dunaliella salina* and transferred to a 26 °C incubator with a 16/8 h light/dark cycle to trigger reproduction. Cultures were monitored daily and when reproduction occurred, juveniles were stored at 18 °C and transferred to experimental conditions within 1–3 days. With a rapid addition of chambers in these first days after reproduction, it is unavoidable that the specimens that were incubated already added a few chambers; inspection revealed that these were never more than five chambers.

Experimental incubation took place at a constant temperature of 24 °C. All juveniles were exposed to a 12 h light/dark cycle (~180 µmol photons m^{-2} s^{-1}). Juveniles were incubated in 200 mL tissue culture flasks in one out of four incubators with its own, constant pCO_2 set to a target value of 400, 800, 1,200 or 1,600 ppm (Fig. 1). In these incubators, pCO_2 was kept as close to the set target value as possible. Inflowing air was scrubbed using soda lime to remove any CO_2 and mixed with pure CO_2 to achieve the target experimental pCO_2 value. Inside the incubator, pCO_2 was constantly monitored and

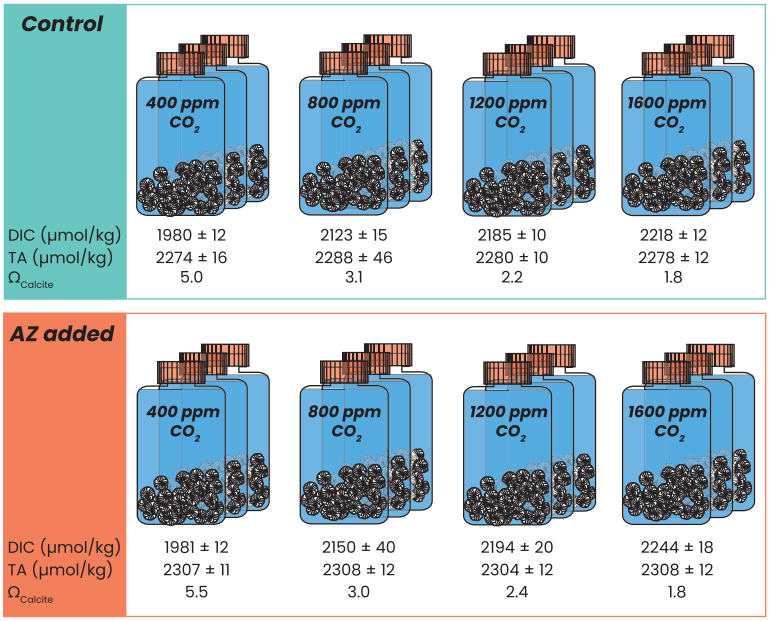

Figure 1 Experimental setup. Schematic overview of all incubations with pCO_2 ranging from 400 to 1,600 ppm, in control (blue) conditions and with 8 µM AZ (in orange), carried out in triplicate per condition. Every flask contained 30–40 specimens of *Amphistegina lessonii*. Measured DIC and TA are indicated below each triplicate, including the calculated saturation state with respect to calcite.
Full-size DOI: 10.7717/peerj.18458/fig-1

the balance of the incoming CO_2-free air: pure CO_2 was automatically adjusted (*Dämmer et al., 2023*). Throughout the experiment, measured pCO_2 varied within ±30 ppm (maximum deviation) of the target value. To prevent evaporation of the culture media, inflowing air was saturated with water by bubbling it through MilliQ before entering the incubator.

Before each experiment, culture flasks containing 200 mL North Atlantic seawater (NASW with a salinity of 36) were allowed to equilibrate at set experimental pCO_2 conditions for between 24 h and several weeks. Following reproduction, 30–40 juvenile specimens were placed into each of these pre-equilibrated flasks. For the control conditions, the flasks contained only sea water and the juvenile specimens. For the experimental conditions, 18 µL of 90 mM acetazolamide (AZ) dissolved in DiMethyl SulfOxide (DMSO) was added to each flask at the start of incubation, resulting in a final AZ concentration of 8 µM. For each condition, incubation was carried out in triplicate, resulting in the incubation of 90–120 specimens per condition (Fig. 1).

The culture media were replaced with fresh, pre-equilibrated sea water twice during the incubation period: after 2 and 4 weeks. After 2 weeks, the incubated juveniles were also fed living *D. salina*. Before feeding, the *D. salina* culture was washed three times with NASW, each time centrifuging for 3 min at 3,000 RPM. *A. lessonii* were fed 200 µL *D. salina* suspension. After 4 weeks, the water was changed once more, and no food was added since the bottoms of all flasks still visibly contained algae. After 5 weeks, the incubation was terminated by submerging the foraminifera in MilliQ. Thereafter, specimens were left to dry and stored at 4 °C until further analysis.

Alkalinity, DIC and nutrient analysis

Dissolved inorganic carbon (DIC), total alkalinity (TA) and nutrient samples of the incubation medium were collected after 2, 4 and 5 weeks of incubation. For DIC measurements, 12 mL of culture media were taken, poisoned with 15 µL $HgCl_2$ and stored in airtight vials at 4 °C until analysis. DIC measurements were carried out on a QuAAtro Continuous Segmented Flow Analyzer (*Stoll et al., 2001*), with an analytical error of ~2.5 µM. For TA, 5 mL subsamples poisoned with $HgCl_2$, were analysed on a QuAAtro Continuous Segmented Flow Analyzer (*Sarazin, Michard & Prevot, 1999*), with typical analytical error of <0.5% of the average. For nutrient analysis, 5 mL samples were taken and stored at −18 °C. Nutrient concentrations for PO_4, NH_4, NO_2 and NO_3 were analyzed on a TrAAcs 800 autoanalyzer (*Murphy & Riley, 1962*; *Helder & De Vries, 1979*; *Grasshoff, Kremling & Ehrhadt, 1999*). For these analyses, a nutrient cocktail was used to monitor precision, showing reproducibility better than 1.5%, but typically 0.7% from the average. Other carbonate system parameters (pH, pCO_2, and carbonate speciation) were calculated using PyCO2SYS (*Humphreys et al., 2022*).

LA-ICP-MS preparation and measurement

After incubation, all specimens underwent an oxidative cleaning treatment to remove organic matter. For each replicate, foraminifera were transferred to a 0.5 mL Eppendorf tube, resulting in a total amount of 30–40 specimens per tube. To each tube, 250 µL freshly prepared alkali buffered 0.33% H_2O_2 solution in 0.5M NH_4OH (0.5 ml and 49.5 ml, respectively) was added. All tubes were then heated in a water bath at 95 °C for 10 min, and placed in an ultrasonic bath (80 kHz, 50% power) for 30 s. These steps were repeated twice. Afterwards, all samples were rinsed three times with MilliQ and dried before analysis.

Elemental ratios in the calcite formed during the incubation period (5–15 chambers) were measured using Laser Ablation Inductively Coupled Plasma Mass Spectrometry (LA-ICP-MS). To ensure that the measured chambers were formed during the incubation period, the laser was focused on each of the final three chambers of specimens cultured under control conditions, and on the final chamber of specimens cultured with AZ.

For the control incubations, 10 specimens for each replicate per pCO_2 were analyzed, resulting in a total of 120 measured specimens. For the specimens incubated with AZ, 10 specimens of only one replicate per pCO_2 were measured (40 specimens total, 10 per replicate), due to the reduced growth in this treatment. Cleaned specimens were placed on a stub with double-sided tape. Chambers were ablated with in a NWR193UC TV2 dual-volume chamber using a circular laser (193 nm) spot with a diameter of 60 µm and a pulse repetition of 6 Hz and an energy density of 1.00 ± 0.05 Jcm^{-2}. The aerosol produced during the ablation was transported to a quadrupole ICP-MS (Thermo Fisher Scientific iCAP-Q; Thermo Fisher Scientific, Waltham, MA, USA) on a helium flow with a flow rate of 0.6 L min^{-1}, with 0.4 L min^{-1} argon make-up gas being added before entering the ICP torch. Elemental quantification was based on cosmic relative abundances of the isotopes considered and using NIST SRMs 612 and 610 (*Jochum et al., 2011*) and using matrix matched standards MACS3, JcT and JcP and NFHS2-NP. At the start of each series and

after every 10–15 samples, the NIST SRM 610 was analyzed. Intensities from the N610 were used to convert the mass intensity ratios (w/t Ca) of the samples to mol/mol.

NFHS-2-NP standard was used to monitor drift after every fourth sample. NFHS-2-NP is the preferred homogeneous reference material for drift monitoring at NIOZ as it shows lower gas blanks for some elements (*e.g.*, Na) than NIST SRM 610 (*Boer et al., 2022*). The calibrated data of NFHS-2-NP using NIST SRM 610 without drift correction were used to calculate drift correction factors (*i.e.*, cps *vs* time) over the course of one run. The first four NFHS-2-NP standards directly measured after the calibration standards were assumed to undergo no drift (*i.e.*, their average intensity was 100%). Although instrumental drift was small, drift corrections were made to improve the accuracy.

The following mass ratios were measured for element quantification: $^{23}Na/^{43}Ca$, $^{25}Mg/^{43}Ca$, $^{88}Sr/^{43}Ca$. Repeatability, *i.e.*, variation in the NFHS2-NP was 2.4% (RSD) for Na/Ca, 0.9% for Mg/Ca, and 0.8% for Sr/Ca. Accuracy was between 99% and 101% for Na/Ca, Mg/Ca and Sr/Ca based on repeated measurements of the MACS3 standard. Throughout the ablation photographs of the ablation spot were taken at 2 s intervals. Ablation profiles were analyzed in MATLAB and examined next to these photographs. The interval selected for elemental quantification was automatically assigned based on the period during which an increase and decrease in Ca was observed (begin and end shell carbonate during ablation). These intervals were later manually adjusted when needed to ensure that the measured interval corresponded to the time period during which ablation photographs showed a hole appearing in the foraminiferal shell wall. Ablation profiles were excluded when the photographs showed no hole appearing during the ablation period, or when no convincing window of Ca increase and subsequent decrease could be detected.

Size

To estimate the size of the cultured specimens, cleaned specimens were placed on a scaled microscope slide and photographed using a stereomicroscope. The cross-sectional area of these specimens was determined using dedicated software (Fiji, DOI: 10.1038/nmeth.2019). Pictures were converted to eight-bit and the pixel value cut-off threshold was adjusted manually to ensure that the chosen threshold corresponded to the specimen's outline. In cases where the lighting made this difficult, specimens' outlines were traced manually. All pictures were then converted to binary images and converted to mask. Using the scale on the pictures, size analysis was carried out using the 'Analyze Particles' module within the Fiji software (size 0.05-Infinity, circularity 0.05–1.00) for the control specimens, and 'Analyze Particles' (size 0.005–Infinity, circularity 0.05–1.00) for specimens incubated with AZ.

Statistical analysis

To assess the (dis)similarity between replicates, an analysis of the difference between the means was carried out for all replicates of each condition. Within each experimental condition, a Shapiro-Wilk analysis was carried out on each replicate to check if data was distributed normally. A Levene test was conducted to assess equality of variance between

replicates. For TA, two pairs of replicates (1,200 ppm CO_2/AZ added; 400 ppm CO_2/control) had slightly different average values (t-test assuming unequal variances, $p < 0.05$); for the DIC analysis, one pair within a treatment had significantly different average values (1,600 ppm CO_2/AZ added). For the nutrient concentrations there were no significant differences in the average concentrations between the replicates within any of the eight treatments (t-test assuming unequal variances, $p > 0.05$ in all cases).

To test for the effect of pCO_2 on El/Ca, we performed an ordinary least sum of squares (OLS) regression analysis assuming a linear response model. This was done in python using the 'statsmodels' library with CO_2 as the independent and El/Ca as the dependent variable.

As the majority of the data did not follow a normal distribution, non-parametric methods were used for further data analysis. This was done for both end size analysis and LA-ICP-MS results. For LA-ICP-MS, outliers were identified using the interquartile range (IQR). If data points fell outside of ±1.5 * IQR, and visual inspection of the LA-ICP-MS depth profile indicated an error in the measurements, the data points were excluded from further analysis. This resulted in the exclusion of 12 out of 120 data points for the control group and three out of 38 data points for the AZ group.

To relate the obtained Mg/Ca to Na/Ca, a regression analysis was performed. This analysis was done using an ordinary least sum of squares (OLS) assuming a power function ($Na/Ca = a * e^{Mg/Ca} + b$). We use the package for Python "scipy" with the module "curvefit" (*Virtanen et al., 2020*). We report the *p*-values of the correlations and the equations, based on correlating Mg/Ca and Na/Ca of all conditions. We calculated the mean and standard errors (SE) for the regression parameters and the shown confidence intervals were calculated from these standard errors.

Comparison between solution- and LA-ICP-MS data

To test the effect of laser ablation (LA) on the obtained Na/Ca, Mg/Ca and Sr/Ca, we measured a number of specimens after dissolution using a sector field-ICP-MS (Element2; Thermo Scientific, Waltham, MA, USA). To do this a volume of 30 µL from every sample was pre-scanned for its calcium concentration ($[Ca^{2+}]$). Based on this pre-scan, all samples' element concentrations were determined from matched $[Ca^{2+}]$. For boron, magnesium and strontium, masses (^{11}B, ^{25}Mg and ^{88}Sr, respectively) were measured in low resolution, whereas sulfur (mass 32) was analyzed in medium resolution to avert interference by $^{16}O^{16}O$. Iron (^{56}Fe) was measured at high resolution to avoid interference of $^{16}O^{40}Ar$. In all samples, ^{43}Ca was monitored to calculate the elemental ratios. This was done using known cosmic relative abundances. Measured samples alternated with 0.1 $MHNO_3$ during the runs for effective wash-out and to avoid carry-over of between samples. All samples were compared to five ratio calibration standards (*De Villiers, Greaves & Elderfield, 2002*). To monitor drift throughout measurements, we included together with three additional standards: NFHS-2-NP (*Boer et al., 2022*), JCt (*Tridacna gigas* giant clam; S/Ca = 0.57 ± 0.04 mmol/mol, B/Ca = 0.23 ± 0.01 mmol/mol, Mg/Ca = 1.21 ± 0.01 mmol/mol, $n = 7$, ± indicates 1 1σ SD) and JCp (*Porites* sp. coral; S/Ca = 5.79 ± 0.14 mmol/mol, B/Ca = 0.50 ± 0.01 mmol/mol, Mg/Ca = 4.05 ±

0.04 mmol/mol, n = 7, ± indicates 1 1σ SD). Since the number of replicates was small for the solution-ICP-MS data and since there were no trends of El/Ca with pCO_2, the El/Ca for the four conditions (both control and when AZ was added) were pooled. A t-test assuming equal variances and $\alpha = 0.05$ showed no significant differences in the averages of Na/Ca and Sr/Ca between the two types of analysis. For Mg/Ca, solution-ICP-MS ratios were slightly lower than the LA-ICP-MS obtained ratios (Tables S2 and S3).

Rayleigh distillation model

To test if the observed trend in Na/Ca and Mg/Ca may be explained by Rayleigh distillation, a simple model was constructed. Ions of magnesium, calcium and sodium are assumed to be incorporated from a fluid with a finite volume into a calcite crystal. The partition coefficient for Mg and Na are described by:

$$K_{Mg} = \left([Mg^{2+}]/[Ca^{2+}]_{calcite}\right)/\left([Mg^{2+}]/[Ca^{2+}]_{fluid}\right) \quad (1)$$

where K_{Mg} is the partition coefficient for magnesium, which is proportional to the ratio of the concentrations of Mg^{2+} and Ca^{2+} in the calcite, divided by that ratio in the fluid from which the $CaCO_3$ precipitates.

If incorporation removes Mg^{2+} and Ca^{2+} in a fixed ratio from a finite volume, the ratio of those two ions remaining in the fluid changes. This is the simplest form of Rayleigh distillation and is described by Eq. (2):

$$D_{Mg} = (1 - f^{KMg})/(1 - f) \quad (2)$$

where D_{Mg} is the distribution coefficient for magnesium and f the fraction of the Ca remaining in the reservoir. If f is close to 1, almost no ions are precipitating from the fluid, while f = 0 indicates that all calcium ions are removed from the calcifying reservoir. In case of the latter, distribution coefficients are close to 1; with a large fraction remaining, distribution coefficients are close the partition coefficients ($D_{Mg} \approx K_{Mg}$). The partition coefficient (K) is here approximated by the partitioning of an ion during inorganic $CaCO_3$ precipitation and is determines part of the overall seawater-foraminiferal calcite partitioning (D). The difference between D and K can be seen as the cellular controls that create a calcifying fluid in which the ions' concentrations are different than those in seawater.

For Na, we assume that Eqs. (1) and (2) are similar. With a system with both Mg and Na being incorporated into the calcite, the ratio of the two ions in the calcite is a function of the ratio of K_{Mg} and K_{Na}. Since these coefficients are also affected by precipitation rate, presence of other ions/organic compounds, $CaCO_3$ phase transformations, *etc*., we used a range of inorganic partition coefficients to calculate the ratio of foraminiferal Mg/Ca *vs* Na/Ca, which essentially reflects the ratio between the inorganic partition coefficients. This is because the factor f (Eq. (2)) has to be the same for both Mg- and Na-incorporation. Since the (initial) composition of the calcifying fluid is essentially unknown, we assume a ten-fold higher (Ca^{2+}) then seawater at the site of calcification. This remains a rough estimate, but an enrichment relative to seawater is likely given the $2H^+/Ca^{2+}$ exchange during calcification for rotaliid foraminifera (*Toyofuku et al., 2017*).

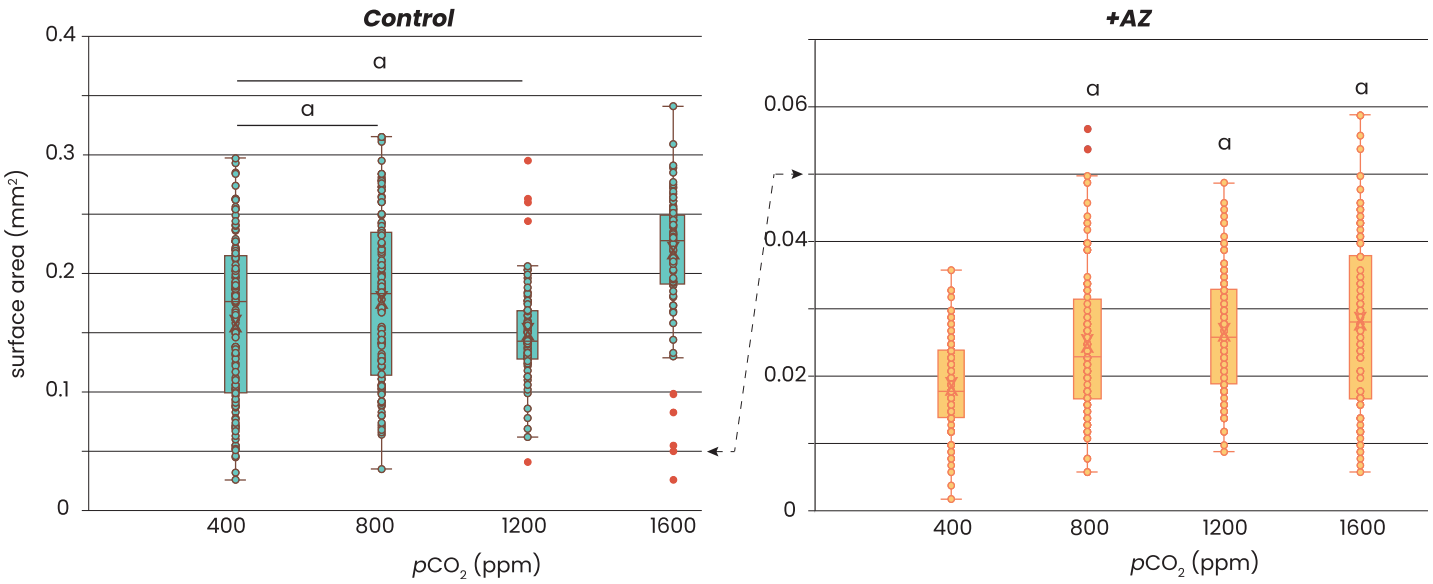

Figure 2 Relation between foraminiferal growth and CO_2. Recorded size of the foraminifera cultured at different pCO_2's is plotted without (left) and with addition of AZ (right): note the difference in the scale of the y-axis. Dots indicate individual foraminifera: outliers are indicated in red and are lower than 1.5 times the lower quartile or higher than 1.5 times the third quartile. Box-whisker plots indicate the average ('X'), the median (horizontal line) and the first and third quartile. An 'a' on top of the box plots indicate which combinations (left) or which treatments (right) are not significantly different from each other (two-tailed t-test, $p < 0.05$). Full-size DOI: 10.7717/peerj.18458/fig-2

RESULTS

Addition of AZ reduced growth of the foraminifera (Fig. 2). Without AZ, specimens grew approximately 8 times larger than the foraminifera incubated with the AZ. Within each of the two treatments, there was no consistent trend in growth (expressed as area of the foraminiferal shell photo's) with pCO_2. For the control groups (*i.e.* no AZ added), only those cultured at highest pCO_2 were significantly larger (t-test, p-value > 0.05) than those at lower CO_2's, while those grown at pCO_2's of 400–1,200 were not significantly different from each other (t-test, p-value > 0.05). For the foraminifera that were incubated with AZ, only those cultured at a pCO_2 of 400 ppm were significantly smaller (t-test, p-value < 0.05) than those incubated at the other pCO_2's. The sizes of the foraminifera from 800, 1,200 and 1,600 ppm CO_2 were not significantly different from each other (t-test, p-value > 0.05).

Element incorporation was also significantly different in the experiments in which AZ was added. Foraminifera grown with AZ have 3 times more Mg in their shell than the specimens grown without AZ (Fig. 3). For Na/Ca, this effect was smaller, with twice as high ratios with than without the inhibitor added. Sr/Ca was least affected by presence of AZ, with about 10% higher Sr/Ca values in case AZ was added. The effect of pCO_2 on element incorporation was absent for all three El/Ca when AZ was added. In the presence of AZ, only Mg/Ca increases linearly with pCO_2 (OLS regression, $p < 0.05$).

Indicated are the Mg/Ca (top), Na/Ca (middle) and Sr/Ca (lower panel) of newly grown chambers from four different pCO_2s. Specimens cultured without addition of AZ are in blue, with addition of AZ in orange. Box-whisker plots indicate the average ('X'), the median (horizontal line) and the first and third quartile. Dots indicate individual

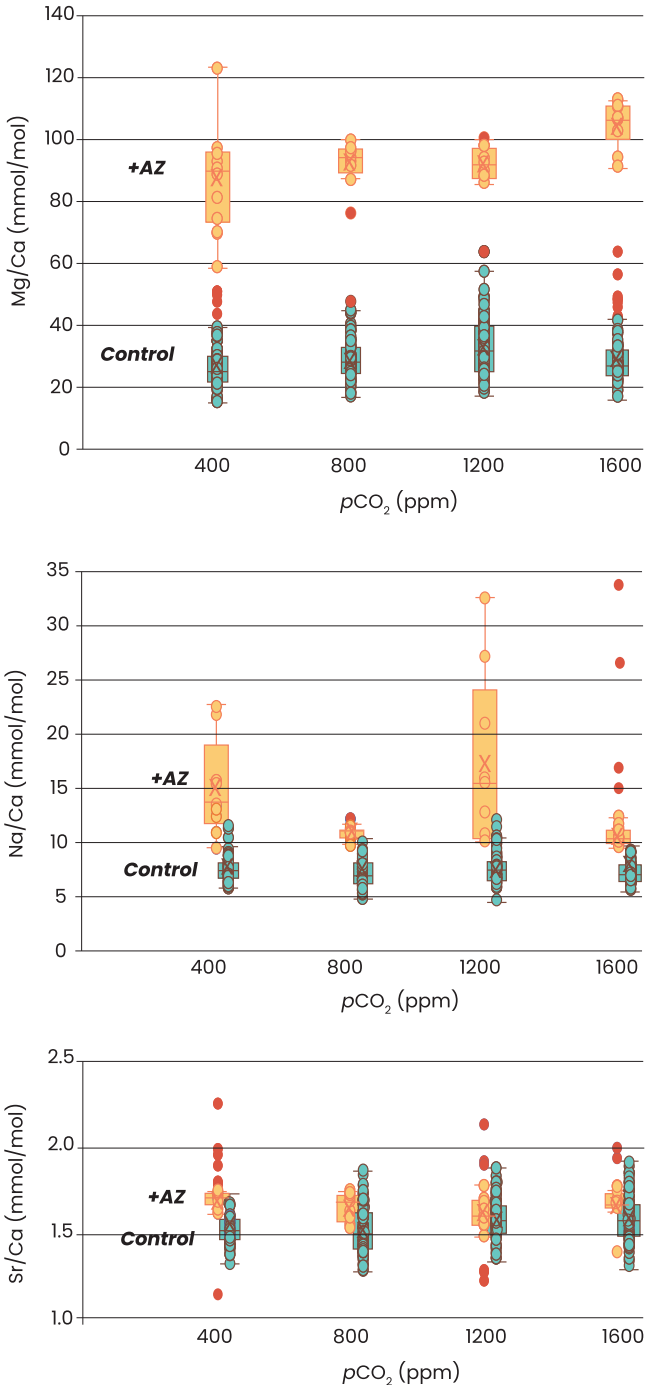

Figure 3 Elemental ratios as a function of CO_2. Recorded size of the foraminifera cultured at different pCO_2's is plotted without (left) and with addition of AZ (right): note the difference in the scale of the y-axis. Dots indicate individual foraminifera: outliers are indicated in red and are lower than 1.5 times the lower quartile or higher than 1.5 times the third quartile. Box-whisker plots indicate the average ('X'), the median (horizontal line) and the first and third quartile. An 'a' on top of the box plots indicate which combinations (left) or which treatments (right) are not significantly different from each other (two-tailed t-test, $p < 0.05$).
Full-size DOI: 10.7717/peerj.18458/fig-3

foraminifera: outliers are indicated in red and are lower than 1.5 times the lower quartile or higher than 1.5 times the third quartile. The two treatments are horizontally shifted in the lower two panels to show the full scale of variability in each of them.

DISCUSSION

Growth rate is affected by AZ and by pCO_2

The clear effect of AZ on growth in *Amphistegina lessonii* (Fig. 2) indicates that conversion between bicarbonate and carbonate by Carbonic Anhydrase (CA) is somehow necessary for growth by foraminifera. This confirms an earlier culturing experiment with foraminifera (*De Goeyse et al., 2021*) and is in line with the importance of CA in calcification in other marine organisms (*e.g.*, corals: *Moya et al., 2008*; bivalves: *Cardoso et al., 2019*). Earlier work on the role of CA on calcification in *Amphistegina* showed that addition of this enzyme reduces calcification (and stimulates photosynthesis; *Ter Kuile, Erez & Padan, 1989*). This led to the conclusion that CA harms calcification, for example by reducing the content of intracellular carbon pools. Results in the same work showed, however, that calcification was also negatively impacted after addition of the CA-inhibitor ethoxyzolamide, indicating that both reduced and increased CA activity are detrimental for inorganic carbon uptake.

The involvement of CA in foraminiferal calcification indicates that they do not (primarily) rely on the available (CO_3^{2-}) in the surrounding seawater. The uptake of bicarbonate and/ or CO_2 and subsequent conversion into CO_3^{2-} at the site of calcification is consistent with biomineralization models that highlighted pH regulation (*e.g.*, *De Nooijer et al., 2009*; *Toyofuku et al., 2017*). Fluorescent labelling showed that during calcification, protons are pumped out of the site of calcification and into the surrounding seawater (*De Nooijer, Toyofuku & Kitazato, 2009*; *Glas, Langer & Keul, 2012*; *Toyofuku et al., 2017*), shifting the inorganic carbon speciation towards CO_2 outside the foraminifera and towards CO_3^{2-} inside the foraminifera, which facilitates inward CO_2 diffusion. Both inside and outside the foraminifer, conversion between inorganic carbon species would benefit from the presence of CA (Fig. 4).

The conversion of CO_2 into HCO_3^- and vice versa is approximately 10^7 times faster in the presence of CA than in its absence (*Zeebe & Wolf-Gladrow, 2001*; *Bertucci et al., 2013*). The conversion of bicarbonate to CO_2 is particularly slow (with kinetics in the ~15 s range) and therefore the aid of CA in this reaction is largest. If foraminifera rely on diffusion of CO_2 from the seawater into the site of calcification, the conversion outside the foraminifers (HCO_3^- -> CO_2) could particularly benefit from the catalysis by CA. Since AZ is membrane-permeable (*Supuran & Scozzafava, 2004*), the effect of AZ could also indicate the presence of CA inside the cell, at the site of calcification, where it may help the conversion of CO_2 into CO_3^{2-} (Fig. 4).

When rotaliid foraminifera calcify, a thin layer of cell material (the protective envelope) separates the calcifying fluid from the surrounding seawater. Within the site of calcification, conditions are manipulated by transport of ions to promote calcium carbonate precipitation (left side). In addition, ions are also transported into the calcifying fluid by vacuolization of seawater (right). The exact ion transport mechanisms, the balance

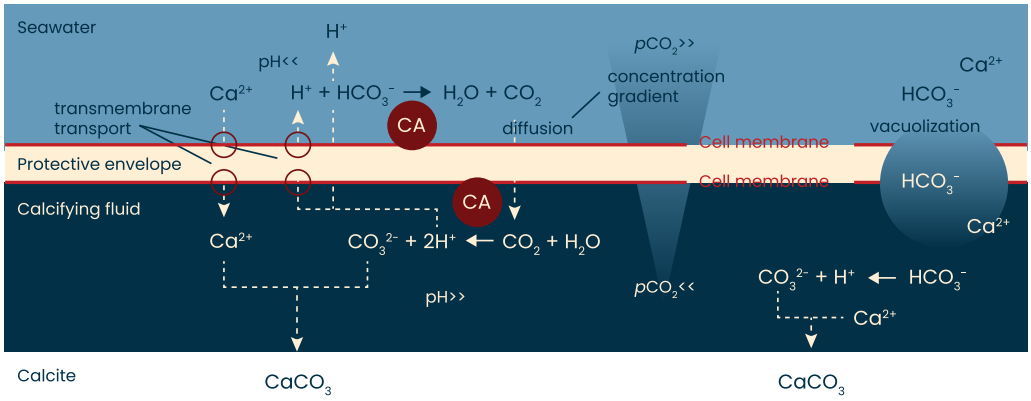

Figure 4 A simplified model of calcification in foraminifera. When rotaliid foraminifera calcify, a thin layer of cell material (the protective envelope) separates the calcifying fluid from the surrounding seawater. Within the site of calcification, conditions are manipulated by transport of ions to promote calcium carbonate precipitation. The exact ion transport mechanisms, the volume of the calcifying fluid, as well as the thickness of the protective envelope remain to be identified and quantified, respectively. Previous work has shown, however, that during calcification protons are pumped from the calcifying fluid to the surrounding seawater. The resulting pH gradient (high inside the calcifying fluid, low outside the foraminifer) will create a pCO_2 gradient that will remain as long as the indicated reactions proceed. Indicated in red are the hypothesized locations of the enzyme carbonic anhydrase (CA): one near the outer cell membrane of the protective envelope and one near the inner membrane. Schematic based on *Erez (2003)*, *Toyofuku et al. (2017)* and *Pacho et al. (2024)*. Full-size DOI: 10.7717/peerj.18458/fig-4

between transmembrane transport and vacuolization, the volume of the calcifying fluid, as well as the thickness of the protective envelope remain to be identified and quantified, respectively. The protons that are pumped from the calcifying fluid to the surrounding seawater result in a pH gradient (high inside the calcifying fluid, low outside the foraminifer) and hence leads to a pCO_2 gradient that will remain as long as the indicated reactions proceed. Presence of symbionts and contribution from respiration may well affect the pH gradient and thus affect the diffusion of CO_2 into the site of calcification. Indicated in red are the hypothesized locations of the enzyme carbonic anhydrase (CA): one near the outer cell membrane of the protective envelope and one near the inner membrane. Schematic based on *Erez (2003)*, *Toyofuku et al. (2017)* and *Pacho et al. (2024)*.

The results from our controlled growth experiments show that there is a small, but positive effect of CO_2 on growth in *Amphistegina lessonii* (Fig. 2), which is in line with earlier experiments (*Dämmer et al., 2023*). Either the lowest set CO_2 conditions resulted in smaller specimens (with AZ) or the highest CO_2 resulted in specimens growing larger shells (without AZ). This suggests that foraminifera do not rely on (CO_3^{2-}) itself, since this would have resulted in a decrease with increasing pCO_2 values (as in sea urchin larvae: *Matt, Chang & Hu, 2022*). The observed positive effect of pCO_2 on calcification is consistent with the active regulation of pH at the site of calcification by foraminifera. The implication of such a mechanism is that an increase in the total dissolved inorganic carbon (DIC) availability, regardless of the ratio between inorganic carbon species, potentially enhances calcification by increasing the DIC pool available to be actively converted into (CO_3^{2-}). Such a positive effect of (DIC) or pCO_2 on calcification in foraminifera has been shown before (*e.g.*, *Hikami et al., 2011*; *Fujita et al., 2011*; *Vogel & Uthicke, 2012*; *Dämmer*

et al., 2023), although other studies also showed a decrease in calcification rates at elevated CO_2 levels (*Allison et al., 2010*; *Barker & Elderfield, 2002*; *Bijma, Spero & Lea, 1999*; *Bijma, Hönisch & Zeebe, 2002*; *Dissard et al., 2010*; *Gonzalez-Mora, Sierro & Flores, 2008*; *Keul et al., 2013*; *De Moel et al., 2009*; *Oron et al., 2020*).

The observed discrepancy may reflect the ability or degree to which extent a species is capable to regulate their internal pH. Strong *vs* weak pH regulation has also been hypothesized to explain variability among marine metazoa to cope with ocean acidification (*Ries, 2011*). Within foraminifera, pH regulation likely also varies between species (*De Nooijer et al., 2023*), explaining the variability in the responses to elevated CO_2. An analysis of the presence and location of carbonic anhydrase among foraminiferal species could help to better understand the interplay between pH regulation, inorganic carbon utilization, photosynthesis and shell chemistry.

Impact of AZ and CO_2 on Mg/Ca, Na/Ca and Sr/Ca

The interplay between calcification and CA is evident from the large impact on the Mg/Ca of newly precipitated calcite after addition of AZ (Fig. 3). When AZ is added the relatively limited amount of carbonate precipitated has much higher Mg/Ca values. The fact that AZ slows down growth (Fig. 2) implies that the increased Mg/Ca ratios are not caused by higher precipitation rates (as shown in inorganic precipitation experiments; *Burton & Walter, 1991*; *Mavromatis et al., 2015*). Although growth by a foraminifer is not necessarily the best predictor for calcite crystal's precipitation rate, it is unlikely that slow rates of chamber addition (Fig. 2) and thin foraminiferal chamber walls are accomplished by higher precipitation rates. Instead, the hampered uptake of inorganic carbon by the inhibition of CA by the added AZ indicates a close coupling between the uptake of the cat- and anions necessary for calcification, assuming an equivalent proportion of high- and low-Mg/Ca bands within the shell walls. With CA being inhibited, affecting bicarbonate-carbonate ion conversions, either Mg uptake is enhanced or Ca intake reduced: the heterogenous distribution of Mg (and other ions) within the shell's wall may provide an explanation for the elevated Mg/Ca at reduced CA activity.

Incorporated elements like S, Ba, Mg, Na, *etc.* within foraminiferal shell walls have been shown to alternate between high-and low-concentration bands (*Kunioka et al., 2006*; *Spero et al., 2015*; *Fehrenbacher et al., 2017*; *Geerken et al., 2019*). Elevated Mg/Ca, S/Ca, *etc.* often coincide with the first layers precipitated, which can be close to the primary organic layer of a new chamber or the layer formed on top of a pre-exiting chamber (*Tyszka et al., 2021*), as is typical for rotaliid species (*Reiss, 1957*; *Erez, 2003*). In the planktonic *Orbulina universa* (*Spero et al., 2015*) and *Neogloboquadrina dutertrei* (*Fehrenbacher et al., 2017*), this high/low banding is shown to be modulated by day/night cyclicity. Irrespective of the environmental trigger(s), incorporated magnesium, strontium, *etc.* and their layered occurrence are likely resulting from a combination of two different proposed modes of calcification: seawater transport and selective, transmembrane ion transport.

Toyofuku et al. (2017) hypothesized that in low-Mg/Ca rotaliid foraminifera, the observed outward proton pumping (from the site of calcification; *De Nooijer et al. (2009)* to the surrounding seawater; *Glas, Langer & Keul, 2012*) is proportional to an inward Ca^{2+}

flux (*Nehrke et al., 2013*) and hence the flux of DIC from the seawater to the site of calcification. The inward diffusion of CO_2, due to the steep site of calcification-seawater pH gradient (approximately 9 to 6; *De Nooijer et al. (2009)* and *Glas, Langer & Keul (2012)*, respectively), provides the necessary protons to maintain the exchange of two protons (out) for one calcium ion (in). It should be noted that the site of calcification likely has a very small volume (*e.g.*, *Nagai et al., 2018*) so that fluxes to the site of calcification will lead to high levels of oversaturation. In addition, it may be that it enters the site of calcification by the Ca^{2+} channel or -pump (*De Nooijer et al., 2014*) because of the Ca pump not being able to discriminate perfectly against Mg (see *Dubicka et al., 2023* for visualization of Ca^{2+} and Mg^{2+} within foraminiferal cells).

Alternatively, seawater vacuolization may supply ions like Mg^{2+} to the site of calcification (*Erez, 2003*; *Bentov & Erez, 2006*; *Bentov, Brownlee & Erez, 2009*). For *Amphistegina*, studies have suggested a relatively large internal ion pool, fueled by seawater uptake prior to calcification (*Ter Kuile & Erez, 1988*). This may mean that the large internal-external pH (and thereby pCO_2) gradient is smaller in *Amphistegina* than described before (*De Nooijer et al., 2009*; *Glas, Langer & Keul, 2012*). It may well be that both modes of ion supply are responsible for the average El/Ca, as well as their layered pattern. The start of chamber formation is likely accompanied by enclosure of seawater, containing Mg^{2+}, Na^{+}, *etc.* that are incorporated during chamber formation (*Geerken et al., 2022*). Incorporation of these elements, plus the subsequent dilution by selective Ca^{2+}-pumping will lower the ratio of (*e.g.*,) Mg^{2+} relative to Ca^{2+} (and thus the Mg/Ca in the calcifying fluid) and result in a lower-concentration band formed after the first high-concentration band is formed. It has also been hypothesized that Mg^{2+} is selectively removed from the site of calcification (*Bentov & Erez, 2006*), but indications for that are currently lacking. For Sr^{2+}, it is likely that some is co-transported through these Ca-pumps (*Hagiwara & Byerly, 1981*; *Baraibar et al., 2018*). With a disturbance of the calcification process due to inactive CA, walls may become significantly thinner and thus the contribution of this first layer will be larger. This will elevate the average Mg/Ca, but will have less effect on Na/Ca and Sr/Ca (Fig. 3). In general, the banding observed for these latter two elements is less pronounced (Na/Ca; *Bonnin et al., 2016*; *Van Dijk et al., 2019*) or absent (Sr/Ca; *Kunioka et al., 2006*; *Geerken et al., 2019*) and thinner shell walls will thus have less impact on their average concentrations.

Differences in how well-pronounced these bands within the shell wall are, is determined by element-specific inorganic partition coefficients (*e.g.*, *Tesoriero & Pankow, 1996*) and subsequent Rayleigh fractionation during continued calcification (*Elderfield, Bertram & Erez, 1996*). Ions that are easily incorporated into the calcite crystal lattice (*i.e.*, described by a high partition coefficient) will decrease relatively rapidly in the fluid at the site of calcification, compared to ions that fit poorly in calcite. Together with the fraction of the ions remaining in the calcifying fluid (*i.e.*, Rayleigh fractionation; *Elderfield, Bertram & Erez, 1996*; *Evans, Müller & Erez, 2018*), these processes determine the average El/Ca in the precipitated shell wall.

The experiments performed here, in which calcification is blocked, can serve to test the Rayleigh fractionation model for element incorporation in foraminiferal shell calcite,

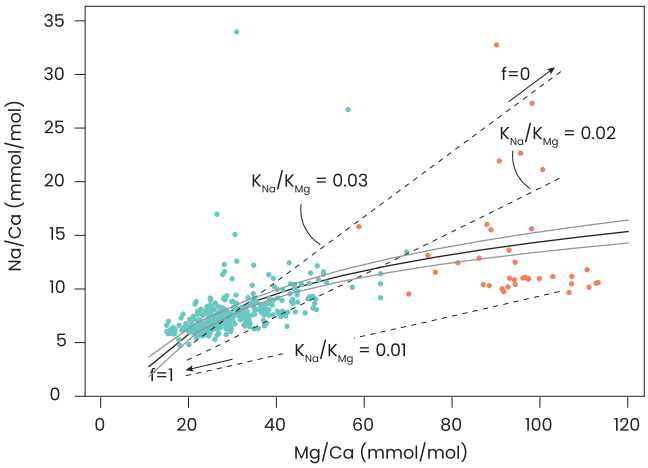

Figure 5 Relation between incorporated Mg and Na. Na/Ca *vs* Mg/Ca in foraminifera grown under control conditions are shown in green and with AZ added in orange. A regression described by Na/Ca = 5.2(±0.39) * $e^{Mg/Ca}$ – 9.7(±1.4) is plotted as a black line with the 95% confidence interval of this regression in grey. Added are dashed lines indicating relations for some combinations of inorganic Mg- and Na-partition coefficients (K_{Mg} and K_{Na}), which are plotted as a function of f (fraction of Ca remaining in the calcifying fluid). The right-hand side of the dashed lines indicate f = 0 (no Ca remains) and the left-hand side f = 1 (almost no $CaCO_3$ precipitates).

Full-size DOI: 10.7717/peerj.18458/fig-5

assuming that the inorganic carbon uptake and calcium pumping are directly coupled. For the inorganic partition coefficients we assumed 0.015–0.020 for magnesium (*Oomori et al., 1987*; *Mucci, 1987*) and 0.0015–0.0025 for Na (*Busenburg & Plummer, 1985*; *DeVriendt et al., 2021*). The relations for the simplified Rayleigh distillation model (Eqs. (1) and (2)) shown in Fig. 4 indicate that the correlation between foraminiferal Mg/Ca and Na/Ca in our dataset can be approximated with a simple Rayleigh fractionation process. Differences between the model outcomes and foraminiferal data (Fig. 4) can be explained by additional controls during biomineralization that may modulate the Mg- and/or Na-partitioning. In particular, a linear trendline through the data would have a non-zero intercept and may indicate that at high values for f, other processes that affect Mg- and Mg-partitioning differently, play a larger role. Such processes may include phase transformations, selective ion transport, precipitation rates, *etc.*

The relatively high spread in El/Ca values in the AZ-treated specimens is likely related to the somewhat larger uncertainty in the analyses caused by the thin shell walls because of the limited amount of carbonate added by the foraminifera under these treatments. Elements in foraminiferal calcite may well be affected by a inward flux of Ca, rather than precipitating from a seawater-like solution. Alternatively, the correlation between El/Ca (Fig. 5) may be explained by distortion of the lattice-strain due to the incorporation of an ion, promoting the incorporation of another one. *Mucci & Morse (1983)* have shown that such an explanation applies to Mg- and Sr-incorporation in inorganically precipitated calcites, while *Evans et al. (2015)* showed the same for Mg- and Na-incorporation. These two hypotheses (Ca-dilution and lattice-strain balancing) do not exclude each other and

future studies will have to show to what magnitude they can explain the correlation between concentrations of elements in foraminiferal calcite.

The effect of the inorganic carbon system on foraminiferal element incorporation showed a negative effect of (CO_3^{2-}) on Mg/Ca (*Dissard et al., 2010*; *Allen et al., 2016*). An experiment with *Amphistegina lobifera*, on the other hand, showed an increase in Mg/Ca with decreasing pH (*Levi, Müller & Erez, 2019*), which is in line with our results (Fig. 3) and results from studies on planktonic species (*Kisakürek et al., 2008*; *Russell et al., 2004*; *Lea, Mashiotta & Spero, 1999*; *Gray & Evans, 2019*). Experiments with several large benthic foraminiferal species, showed no effect of pCO_2 on Mg/Ca, Na/Ca and Sr/Ca (*Van Dijk, De Nooijer & Reichart, 2017*). The combination of these reports and the results shown here suggest that the minor effect of pH/CO_2/(CO_3^{2-}) on Mg incorporation is likely an indirect effect, possibly related to variability in Ca^{2+} pumping rates or the ratio of high- and low-Mg/Ca bands. This underscores the necessity to unravel the foraminiferal calcification pathway when aiming to explain the effect of environmental variables on their calcite's composition.

CONCLUSIONS

Calcification in the benthic foraminifer *Amphistegina lessonii* critically relies on carbonic anhydrase. With the inhibitor acetazolamide added to the culturing medium, sizes of the specimens were 5–10 times smaller than in the control group. The involvement of carbonic anhydrase fits the conversion of bicarbonate into CO_2 and vice versa, as hypothesized in recent models for calcification in foraminifera. The steep increase in the calcite's Mg over Ca concentration after addition of acetazolamide further suggests that Ca-pumping and inorganic carbon uptake are directly coupled and has a major impact on El/Ca values. The positive (although relatively small) effect of increased ambient CO_2 on calcification confirms that foraminiferal pH regulation decouples calcification from the saturation state in the surrounding seawater.

ADDITIONAL INFORMATION AND DECLARATIONS

Funding

This work was supported by the Dutch Research Council (ALWOP210). The funders had no role in study design, data collection and analysis, decision to publish, or preparation of the manuscript.

Grant Disclosures

The following grant information was disclosed by the authors:
Dutch Research Council: ALWOP210.

Competing Interests

The authors declare that they have no competing interests.

Author Contributions

- Siham De Goeyse conceived and designed the experiments, performed the experiments, analyzed the data, prepared figures and/or tables, authored or reviewed drafts of the article, and approved the final draft.
- Chiara Lesuis performed the experiments, analyzed the data, authored or reviewed drafts of the article, and approved the final draft.
- Gert-Jan Reichart analyzed the data, authored or reviewed drafts of the article, and approved the final draft.
- Lennart de Nooijer conceived and designed the experiments, performed the experiments, analyzed the data, prepared figures and/or tables, authored or reviewed drafts of the article, and approved the final draft.

Data Availability

The following information was supplied regarding data availability:

The inorganic carbon chemistry (DIC and TA), as well as the growth and foraminiferal geochemistry, are available in the Supplemental File.

Supplemental Information

Supplemental information for this article can be found online at http://dx.doi.org/10.7717/peerj.18458#supplemental-information.

REFERENCES

Allen KA, Hönisch B, Eggins SM, Haynes LL, Rosenthal Y, Yu J. 2016. Trace element proxies for surface ocean conditions: a synthesis of culture calibrations with planktic foraminifera. *Geochimica et Cosmochimica Acta* **193(C)**:197–221 DOI 10.1016/j.gca.2016.08.015.

Allison N, Austin W, Paterson D, Austin H. 2010. Culture studies of the benthic foraminifera *Elphidium williamsoni*: evaluating pH, $\Delta[CO_3^{2-}]$ and inter-individual effects on test Mg/Ca. *Chemical Geology* **274(1–2)**:87–93 DOI 10.1016/j.chemgeo.2010.03.019.

Anand P, Elderfield H, Conte MH. 2003. Calibration of Mg/Ca thermometry in planktonic foraminifera from a sediment trap time series. *Paleoceanography* **18(2)**:1050 DOI 10.1029/2002PA000846.

Baraibar AM, De Pascual R, Camacho M, Domínguez N, David Machado J, Gandía L, Borges R. 2018. Distinct patterns of exocytosis elicited by Ca^{2+}, Sr^{2+} and Ba^{2+} in bovine chromaffin cells. *European Journal of Physiology* **470(10)**:1459–1471 DOI 10.1007/s00424-018-2166-4.

Barker S, Elderfield H. 2002. Foraminiferal calcification response to glacial-interglacial changes in atmospheric CO_2. *Science* **297(5582)**:833–836 DOI 10.1126/science.1072815.

Bentov S, Brownlee C, Erez J. 2009. The role of seawater endocytosis in the biomineralization process in calcareous foraminifera. *Proceedings of the National Academy of Sciences of the USA* **106(51)**:21500–21504 DOI 10.1073/pnas.0906636106.

Bentov S, Erez J. 2006. Impact of biomineralization process on the Mg content of foraminiferal shells: a biological perspective. *Geochemistry, Geophysics, Geosystems* **7(1)**:1 DOI 10.1029/2005GC001015.

Bertucci A, Moya A, Tambutté S, Allemand D, Supuran CT, Zoccola D. 2013. Carbonic anhydrases in anthozoan corals—a review. *Bioorganic & Medicinal Chemistry* **21(6)**:1437–1450 DOI 10.1016/j.bmc.2012.10.024.

Bijma J, Hönisch B, Zeebe RE. 2002. Impact of the ocean carbonate chemistry on living foraminiferal shell weight: comment on "Carbonate ion concentration in glacial-age deep waters of the Caribbean Sea" by W. S. Broecker and E. Clark. *Geochemistry, Geophysics, Geosystems* **3(11)**:1064 DOI 10.1029/2002GC000388.

Bijma J, Spero HJ, Lea DW. 1999. Reassessing foraminiferal stable isotope geochemistry: impact of the oceanic carbonate system (experimental results). In: Fischer G, Wefer G, eds. *Use of Proxies in Paleoceanography: Examples from the South Atlantic*. Berlin, Heidelberg: Springer-Verlag, 489–512.

Boer W, Norstad S, Weber M, Mertz-Kraus R, Hönisch B, Bijma J, Raitzsch M, Wilhelms-Dick D, Foster GL, Goring-Harford H, Nürnberg D, Hauff F, Kuhnert H, Lugli F, Spero H, Rosner M, Van Gaever P, De Nooijer LJ, Reichart G-J. 2022. New calcium carbonate nano-particulate pressed powder pellet (NFHS-2-NP) for LA-IPC-OES, LA-(MC)-ICP-MS and μXRF. *Geostandards and Geoanalytical Research* **46(3)**:411–432 DOI 10.1111/ggr.12425.

Bonnin EA, Zhu Z, Fehrenbacher JS, Russell AD, Hönisch B, Spero HJ, Gagnon A. 2016. Submicron sodium banding in cultured planktonic foraminifera shells. *Geochimica et Cosmochimica Acta* **253**:127–145 DOI 10.1016/j.gca.2019.03.024.

Burton EA, Walter LM. 1991. The effects of PCO_2 and temperature on magnesium incorporation in calcite in seawater and $MgCl_2$-$CaCl_2$ solutions. *Geochimica et Cosmochimica Acta* **55(3)**:777–785 DOI 10.1016/0016-7037(91)90341-2.

Busenburg E, Plummer LN. 1985. Kinetic and thermodynamic factors controlling the distribution of SO_4^{2-} and Na^+ in calcites and selected aragonites. *Geochimica et Cosmochimica Acta* **49(3)**:713–725 DOI 10.1016/0016-7037(85)90166-8.

Cardoso JCR, Ferreira V, Zhang X, Anjos L, Félix RC, Batista FM, Power DM. 2019. Evolution and diversity of alpha-carbonic anhydrases in the mantle of the Mediterranean mussel (*Mytilus galloprovincialis*). *Scientific Reports* **9**:10400 DOI 10.1038/s41598-019-46913-2.

Chen S, Gagnon A, Adkins JF. 2018. Carbonic anhydrase, coral calcification and a new model of stable isotope vital effects. *Geochimica et Cosmochimica Acta* **236(12)**:179–197 DOI 10.1016/j.gca.2018.02.032.

Dämmer LK, Ivkic A, De Nooijer LJ, Renema W, Webb AE, Reichart G-J. 2023. Impact of dissolved CO_2 on calcification in two large, benthic foraminiferal species. *PLOS ONE* **18(8)**:e0289122 DOI 10.1371/journal.pone.0289122.

Dämmer LK, Van Dijk I, De Nooijer LJ, Van der Wagt B, Wilckens FK, Zoetemelk B, Reichart G-J. 2021. Temperature impact on magnesium isotope fractionation in cultured foraminifera. *Frontiers in Earth Science* **9**:642256 DOI 10.3389/feart.2021.642256.

De Goeyse S, Webb AE, Reichart G-J, De Nooijer LJ. 2021. Carbonic anhydrase is involved in calcification by the benthic foraminifer *Amphistegina lessonii*. *Biogeosciences* **18(2)**:393–401 DOI 10.5194/bg-18-393-2021.

De Moel H, Ganssen GM, Peeters FJC, Jung SJA, Kroon D, Brummer GJA, Zeebe RE. 2009. Planktic foraminiferal shell thinning in the Arabian Sea due to anthropogenic ocean acidification? *Biogeosciences* **6(9)**:1917–1925 DOI 10.5194/bg-6-1917-2009.

De Nooijer LJ, Langer G, Nehrke G, Bijma J. 2009. Physiological controls on the seawater uptake and calcification in the benthic foraminifer *Ammonia tepida*. *Biogeosciences* **6(11)**:2669–2675 DOI 10.5194/bg-6-2669-2009.

De Nooijer LJ, Pacho Sampedro L, Jorissen FJ, Pawlowski J, Rosenthal Y, Dissard D, Reichart GJ. 2023. 500 million years of foraminiferal calcification. *Earth-Science Reviews* **243**:104484 DOI 10.1016/j.earscirev.2023.104484.

De Nooijer LJ, Spero HJ, Erez J, Bijma J, Reichart GJ. 2014. Biomineralization in perforate Foraminifera. *Earth-Science Reviews* **135**:48–58 DOI 10.1016/j.earscirev.2014.03.013.

De Nooijer LJ, Toyofuku T, Kitazato H. 2009. Foraminifera promote calcification by elevating their intracellular pH. *Proceedings of the National Academy of Sciences of the USA* **106(36)**:15374–15378 DOI 10.1073/pnas.0904306106.

De Nooijer LJ, Van Dijk I, Toyofuku T, Reichart G-J. 2017. The impacts of seawater Mg/Ca and temperature on element incorporation in benthic foraminiferal calcite. *Geochemistry, Geophysics, Geosystems* **18(10)**:3617–3630 DOI 10.1002/2017GC007183.

De Villiers S, Greaves M, Elderfield H. 2002. An intensity ratio calibration method for the accurate determination of Mg/Ca and Sr/Ca of marine carbonates by ICP-AES. *Geochemistry, Geophysics, Geosystems* **3(1)**:1001 DOI 10.1029/2001GC000169.

DeVriendt LS, Mezger EM, Olsen EK, Watkins JM, Kaczmarek K, Nehrke G, De Nooijer LJ, Reichart GJ. 2021. Sodium incorporation into inorganic $CaCO_3$ and implications for biogenic carbonates. *Geochimica et Cosmochimica Acta* **314**:294–312 DOI 10.1016/j.gca.2021.07.024.

Dissard D, Nehrke G, Reichart GJ, Bijma J. 2010. The impact of salinity on the Mg/Ca and Sr/Ca ratio in the benthic foraminifera *Ammonia tepida*: results from culture experiments. *Geochimica et Cosmochimica Acta* **74(3)**:928–940 DOI 10.1016/j.gca.2009.10.040.

Dubicka S, Bojanowski MJ, Bijma J, Bickmeyer U. 2023. Mg-rich amorphous to Mg-low crystalline CaCO3 pathway in foraminifera. *Heliyon* **9(7)**:e18331 DOI 10.1016/j.heliyon.2023.e18331.

Elderfield H, Bertram CJ, Erez J. 1996. A biomineralization model for the incorporation of trace elements into foraminiferal calcium carbonate. *Earth and Planetary Science Letters* **142(3–4)**:409–423 DOI 10.1016/0012-821X(96)00105-7.

Erez J. 2003. The source of ions for biomineralization in foraminifera and their implications for paleoceanographic proxies. In: Dove PM, De Yoreo JJ, eds. *Reviews in Mineralogy and Geochemistry*. Vol. 54. Chantilly: Mineralogical Society of America, Geochemical Society, 115–149.

Evans D, Erez J, Oron S, Müller W. 2015. Mg/Ca-temperature and seawater-test chemistry relationships in the shallow-dwelling large benthic foraminifera. *Geochimica et Cosmochimica Acta* **148**:325–342 DOI 10.1016/j.gca.2014.09.039.

Evans D, Müller W, Erez J. 2018. Assessing foraminifera biomineralisation models through trace element data of cultures under variable seawater chemistry. *Geochimica et Cosmochimica Acta* **236**:198–217 DOI 10.1016/j.gca.2018.02.048.

Feely RA, Sabine CL, Lee K, Berelson W, Kleypas J, Fabry VJ, Millero FJ. 2004. Impact of anthropogenic CO_2 on the $CaCO_3$ system in the oceans. *Science* **305(5682)**:362–366 DOI 10.1126/science.1097329.

Fehrenbacher J, Russel AD, Davis CV, Gagnon AC, Spero HJ, Cliff JB, Zhu Z, Martin P. 2017. Link between light-triggered Mg-banding and chamber formation in the planktonic foraminifera *Neogloboquadrina dutertrei*. *Nature Communications* **8(1)**:15441 DOI 10.1038/ncomms15441.

Fujita K, Hikami M, Suzuki A, Kuroyanagi A, Sakai K, Kawahata H, Nojiri Y. 2011. Effects of ocean acidification on calcification of symbiont-bearing reef foraminifers. *Biogeosciences* **8(8)**:2089–2098 DOI 10.5194/bg-8-2089-2011.

Geerken E, De Nooijer LJ, Roepert A, Polerecky L, King HE, Reichart GJ. 2019. Element banding and organic linings within chamber walls of two benthic foraminifera. *Scientific Reports* **9(1)**:3598 DOI 10.1038/s41598-019-40298-y.

Geerken E, De Nooijer LJ, Toyofuku T, Roepert A, Middelburg JJ, Kienhuis MVM, Nagai Y, Polerecky L, Reichart GJ. 2022. High precipitation rates characterize biomineralization in the benthic foraminifer *Ammonia beccarii*. *Geochimica et Cosmochimica Acta* **318**:70–82 DOI 10.1016/j.gca.2021.11.026.

Geerken E, De Nooijer LJ, Van Dijk I, Reichart G-J. 2018. Impact of salinity on element incorporation in two benthic foraminiferal species with contrasting magnesium contents. *Biogeosciences* **15(7)**:2205–2218 DOI 10.5194/bg-15-2205-2018.

Glas M, Langer G, Keul N. 2012. Calcification acidifies the microenvironment of a benthic foraminifer (*Ammonia* sp.). *Journal of Experimental Marine Biology and Ecology* **424–425(2)**:53–58 DOI 10.1016/j.jembe.2012.05.006.

Gonzalez-Mora B, Sierro FJ, Flores JA. 2008. Controls of shell calcification in planktonic foraminifers. *Quaternary Science Reviews* **27(9–10)**:956–961 DOI 10.1016/j.quascirev.2008.01.008.

Grasshoff K, Kremling K, Ehrhadt M. 1999. *Methods of seawater analysis*. Hoboken: Wiley.

Gray WR, Evans D. 2019. Nonthermal influences on Mg/Ca in planktonic foraminifera: a review of culture studies and application to the last glacial maximum. *Paleoceanography and Paleoclimatology* **34(3)**:306–315 DOI 10.1029/2018PA003517.

Hagiwara S, Byerly L. 1981. Calcium channel. *Annual Review of Neuroscience* **4(1)**:69–125 DOI 10.1146/annurev.ne.04.030181.000441.

Haynert K, Schönfeld J, Schiebel R, Wilson B, Thomsen J. 2014. Response of benthic foraminifera to ocean acidification in their natural sediment environment: a long-term culturing experiment. *Biogeosciences* **11(6)**:1581–1597 DOI 10.5194/bg-11-1581-2014.

Helder W, De Vries RTP. 1979. An automatic phenol-hypochlorite method for the determination of ammonia in sea- and brackish waters. *Netherlands Journal of Sea Research* **13(1)**:154–160 DOI 10.1016/0077-7579(79)90038-3.

Hikami M, Ushie H, Irie T, Fujita K, Kuroyanagi A, Sakai K, Nojiri Y, Suzuki A, Kawahata H. 2011. Contrasting calcification responses to ocean acidification between two reef foraminifers harboring different algal symbionts. *Geophysical Research Letters* **38(19)**:L19601 DOI 10.1029/2011GL048501.

Humphreys MP, Lewis ER, Sharp JD, Pierrot D. 2022. PyCO2SYS v1.8: marine carbonate system calculations in Python. *Geoscientific Model Development* **15(1)**:15–43 DOI 10.5194/gmd-15-15-2022.

Jochum KP, Weis U, Stoll B, Kuzmin D, Yang Q, Raczek I, Jacob DE, Stracke A, Birbaum K, Frick DA, Günther D, Enzweiler J. 2011. Determination of reference values for NIST SRM 610-617 glasses following ISO guidelines. *Geostandards and Geoanalytical Research* **35(4)**:397–429 DOI 10.1111/j.1751-908X.2011.00120.x.

Keul N, Langer G, De Nooijer LJ, Bijma J. 2013. Effect of ocean acidification on the benthic foraminifera *Ammonia* sp. is caused by a decrease in carbonate ion concentration. *Biogeosciences* **10(10)**:6185–6198 DOI 10.5194/bg-10-6185-2013.

Kisakürek B, Eisenhauer A, Böhm F, Garbe-Schönberg D, Erez J. 2008. Controls on shell Mg/Ca and Sr/Ca in cultured planktonic foraminiferan, *Globigerinoides ruber* (white). *Earth and Planetary Science Letters* **273(3–4)**:260–269 DOI 10.1016/j.epsl.2008.06.026.

Köhler-Rink S, Kühl M. 2000. Microsensor studies of photosynthesis and respiration in larger symbiotic foraminifera. I The physico-chemical microenvironment of *Marginopora vertebralis*, *Amphistegina lobifera* and *Amphisorus hemprichii*. *Marine Biology* **137(3)**:473–486 DOI 10.1007/s002270000335.

Köhler-Rink S, Kühl M. 2005. The chemical microenvironment of the symbiotic planktonic foraminifer *Orbulina universa*. *Marine Biology Research* **1**:68–78 DOI 10.1080/17451000510019015.

Kunioka D, Shirai K, Takahata N, Sano Y, Toyofuku T, Ujiie Y. 2006. Microdistribution of Mg/Ca, Sr/Ca, and Ba/Ca ratios in *Pulleniatina obliquiloculata* test by using a NanoSIMS: implication for the vital effect mechanism. *Geochemistry, Geophysics, Geosystems* **7(12)**:Q12P20 DOI 10.1029/2006GC001280.

Le Roy N, Jackson DJ, Marie B, Ramos-Silva P, Marin F. 2014. The evolution of metazoan α-carbonic anhydrases and their roles in calcium carbonate biomineralization. *Frontiers in Zoology* **11**:75 DOI 10.1186/s12983-014-0075-8.

Lea DW, Mashiotta TA, Spero HJ. 1999. Controls on magnesium and strontium uptake in planktonic foraminifera determined by live culturing. *Geochimica et Cosmochimica Acta* **63(16)**:2369–2379 DOI 10.1016/S0016-7037(99)00197-0.

Levi A, Müller W, Erez J. 2019. Intrashell variability of trace elements in benthic Foraminifera grown under high CO_2 levels. *Frontiers in Earth Science* **7**:247 DOI 10.3389/feart.2019.00247.

Lindskog S. 1997. Structure and mechanism of carbonic anhydrase. *Pharmacology and Therapeutics* **74(1)**:1–20 DOI 10.1016/S0163-7258(96)00198-2.

Matt A-S, Chang WW, Hu MY. 2022. Extracellular carbonic anhydrase activity promotes a carbon concentrating mechanism in metazoan calcifying cells. *Proceedings of the National Academy of Sciences of the USA* **4(40)**:119 DOI 10.1073/pnas.2203904119.

Mavromatis V, Montouillout V, Noireaux J, Gaillardet J, Schott J. 2015. Characterization of boron incorporation and speciation in calcite and aragonite from co-precipitation experiments under controlled pH, temperature and precipitation rate. *Geochimica et Cosmochimica Acta* **150**:299–313 DOI 10.1016/j.gca.2014.10.024.

Medaković D. 2000. Carbonic anhydrase activity and biomineralization process in embryos, larvae and adult blue mussels *Mytilus edulis* L. *Helgoland Marine Research* **54**:1–6 DOI 10.1007/s101520050030.

Moya A, Ferrier-Pagès C, Furla P, Richier S, Tambutté E, Allemand D, Tambutté S. 2008. Calcification and associated physiological parameters during a stress event in the scleractinian coral *Stylophora pistillata*. *Comparative Biochemistry and Physiology Part A: Molecular & Integrative Physiology* **151(1)**:29–36 DOI 10.1016/j.cbpa.2008.05.009.

Mucci A. 1987. Influence of temperature on the composition of magnesian calcite overgrowths precipitated from seawater. *Geochimica et Cosmochimica Acta* **51**:1977–1984 DOI 10.1016/0016-7037(87)90186-4.

Mucci A, Morse JW. 1983. The incorporation of Mg^{2+} and Sr^{2+} into calcite overgrowths: influences of growth rate and solution composition. *Geochimica et Cosmochimica Acta* **47(2)**:217–233 DOI 10.1016/0016-7037(83)90135-7.

Müller WEG, Schröder HC, Schlossmacher U, Neufurth M, Geurtsen W, Korzhev M, Wang X. 2013. The enzyme carbonic anhydrase as an integral component of biogenic Ca-carbonate formation in sponge spicules. *FEBS Open Biology* **3**:357–362 DOI 10.1016/j.fob.2013.08.004.

Murphy J, Riley JP. 1962. A modified single solution method for the determination of phosphate in natural waters. *Analytica Chimica Acta* **27**:31–36 DOI 10.1016/S0003-2670(00)88444-5.

Nagai Y, Uematsu K, Chen C, Wani R, Tyszka J, Toyofuku T. 2018. Weaving of biomineralization framework in rotaliid foraminifera: implications for paleoceanographic proxies. *Biogeosciences* **15**:6773–6789 DOI 10.5194/bg-15-6773-2018.

Nehrke G, Keul N, Langer G, De Nooijer LJ, Bijma J, Meibom A. 2013. A newmodel for biomineralization and trace-element signatures of foraminiferal tests. *Biogeosciences* **10(10)**:6759–6767 DOI 10.5194/bg-10-6759-2013.

Nürnberg D, Bijma J, Hemleben C. 1996. Assessing the reliability of magnesium in foraminiferal calcite as a proxy for water mass temperature. *Geochimica Cosmochimica Acta* **60(5)**:803–814 DOI 10.1016/0016-7037(95)00446-7.

Oomori T, Kaneshima H, Maezato Y, Kitano Y. 1987. Distribution coefficient of Mg^{2+} ions between calcite and solution at 10–50°C. *Marine Chemistry* **20(4)**:327–336 DOI 10.1016/0304-4203(87)90066-1.

Oron S, Evans D, Abramovich S, Almogi-Labin A, Erez J. 2020. Differential sensitivity of a symbiont-bearing foraminifer to seawater carbonate chemistry in a decoupled DIC-pH experiment. *Journal of Geochemical Research: Biogeosciences* **125(9)**:e2020JG005726 DOI 10.1029/2020JG005726.

Pacho L, De Nooijer LJ, Boer W, Reichart GJ. 2024. Differences between potassium and sodium incorporation in foraminiferal shell carbonate. *Frontiers in Marine Science* **11**:1385247 DOI 10.3389/fmars.2024.1385347.

Raja R, Saraswati PK, Iwao K. 2007. A field-based study on variation in Mg/Ca and Sr/Ca in larger benthic foraminifera. *Geochemistry, Geophysics, Geosystems* **8(10)**:Q10012 DOI 10.1029/2006GC001478.

Raja R, Saraswati PK, Rogers K, Iwao K. 2005. Magnesium and strontium compositions of recent symbiont-bearing benthic foraminifera. *Marine Micropaleontology* **58**:31–44 DOI 10.1016/j.marmicro.2005.08.001.

Reiss Z. 1957. The Bilamellidea, nov. Superfam., and remarks on Cretaceous Globorotaliids. *Contributions from the Cushman Foundation for Foraminiferal Research* **8(4)**:127–145.

Ries JB. 2011. A physicochemical framework for interpreting the biological calcification response to CO_2-induced ocean acidification. *Geochimica et Cosmochimica Acta* **75(14)**:4053–4064 DOI 10.1016/j.gca.2011.04.025.

Rink S, Kühl M, Bijma J, Spero HJ. 1998. Microsensor studies of photosynthesis and respiration in the symbiotic foraminifer *Orbulina universa*. *Marine Biology* **131(4)**:583–595 DOI 10.1007/s002270050350.

Russell AD, Hönisch B, Spero HJ, Lea DW. 2004. Effects of seawater carbonate ion concentration and temperature on shell U, Mg, and Sr in cultured planktonic foraminifera. *Geochimica et Cosmochimica Acta* **68(21)**:4347–4361 DOI 10.1016/j.gca.2004.03.013.

Sabine CL, Tanhua T. 2010. Estimation of anthropogenic CO_2 inventories in the ocean. *Annual Review of Marine Science* **2**:269–292 DOI 10.1146/annurev-marine-120308-080947.

Sadekov AY, Darling KF, Ishimura T, Wade CM, Kimoto K, Singh AD, Anand P, Kroon D, Jung S, Ganssen G, Ganeshram R, Tsunogai U, Elderfield H. 2016. Geochemical imprints of genotypic variants of *Globigerina bulloides* in the Arabian Sea. *Paleoceanography* **31(10)**:1440–1452 DOI 10.1002/2016PA002947.

Sarazin G, Michard G, Prevot F. 1999. A rapid and accurate spectroscopic method for alkalinity measurements in sea water samples. *Water Research* **33(1)**:290–294 DOI 10.1016/S0043-1354(98)00168-7.

Sarmiento JL, Dunne J, Gnanadesikan A, Key RM, Matsumoto K, Slater R. 2002. A new estimate of the $CaCO_3$ to organic carbon export ratio. *Global Biogeochemical Cycles* **16(4)**:54-1–54-12 DOI 10.1029/2002gb001919.

Schiebel R. 2002. Planktic foraminiferal sedimentation and the marine calcite budget. *Global Biogeochemical Cycles* **16(4)**:1065 DOI 10.1029/2001GB001459.

Schmiedl G, Pfeilsticker M, Hemleben C, Mackensen A. 2004. Environmental and biological effects on the stable isotope composition of recent deep-sea benthic foraminifera from the western Mediterranean Sea. *Marine Micropaleontology* **51(1–2)**:129–152 DOI 10.1016/j.marmicro.2003.10.001.

Segev E, Erez J. 2006. Effect of Mg/Ca ratio in seawater on shell composition in shallow benthic foraminifera. *Geochemistey, Geophysics, Geosystems* **7(2)**:Q02P09 DOI 10.1029/2005GC000969.

Spero HJ, Eggins SM, Russell AD, Vetter L, Kilburn MR, Hönisch B. 2015. Timing and mechanism for intratest Mg/Ca variability in a living planktic foraminifer. *Earth and Planetary Science Letters* **409(2)**:32–42 DOI 10.1016/j.epsl.2014.10.030.

Stoll MHC, Bakker K, Nobbe GH, Haese RR. 2001. Continuous-flow analysis of dissolved inorganic carbon content in seawater. *Analytical Chemistry* **73**:4111–4116 DOI 10.1021/ac010303r.

Supuran CT, Scozzafava A. 2004. Benzolamide is not a membrane-impermeant carbonic anhydrase inhibitor. *Journal of Enzyme Inhibition and Medicinal Chemistry* **19(3)**:269–273 DOI 10.1080/14756360410001689559.

Ter Kuile B, Erez J. 1988. The size and function of the internal inorganic carbon pool of the foraminifer *Amphistegina lobifera*. *Marine Biology* **99(4)**:481–487 DOI 10.1007/BF00392555.

Ter Kuile B, Erez J, Padan E. 1989. Competition for inorganic carbon between photosynthesis and calcification in the symbiont-bearing *Amphistegina lobifera*. *Marine Biology* **103(2)**:253–259 DOI 10.1007/BF00543355.

Tesoriero AJ, Pankow JF. 1996. Solid solution partitioning of Sr^{2+}, Ba^{2+}, and Cd^{2+} to calcite. *Geochimica et Cosmochimica Acta* **60(6)**:1053–1063 DOI 10.1016/0016-7037(95)00449-1.

Toyofuku T, Matsuo MY, De Nooijer LJ, Nagai Y, Kawada S, Fujita K, Reichart G-J, Nomaki H, Tsuchiya M, Sakaguchi H, Kitazato H. 2017. Proton pumping accompanies calcification in foraminifera. *Nature Communications* **8**:14145 DOI 10.1038/ncomms14145.

Toyofuku T, Suzuki M, Suga H, Sakai S, Suzuki A, Ishikawa T, De Nooijer LJ, Schiebel R, Kawahata H, Kitazato H. 2011. Mg/Ca and $\delta^{18}O$ in the brackish shallow-water benthic foraminifer Ammonia 'beccarii'. *Marine Micropaleontology* **78(3–4)**:113–120 DOI 10.1016/j.marmicro.2010.11.003.

Tyszka J, Godos K, Golén J, Radmacher W. 2021. Foraminiferal organic linings: functional and phylogenetic challenges. *Earth-Science Reviews* **220(5)**:103726 DOI 10.1016/j.earscirev.2021.103726.

Van Dijk I, Barras C, De Nooijer LJ, Mouret A, Geerken E, Oron S, Reichart G-J. 2019. Coupled calcium and inorganic carbon uptake suggested by magnesium and sulfur incorporation in foraminiferal calcite. *Biogeosciences* **16(10)**:2115–2130 DOI 10.5194/bg-16-2115-2019.

Van Dijk I, De Nooijer LJ, Reichart G-J. 2017. Trends in element incorporation in hyaline and porcelaneous foraminifera as a function of pCO_2. *Biogeosciences* **14(3)**:497–510 DOI 10.5194/bg-14-497-2017.

Virtanen P, Gommers R, Oliphant TE, Haberland M, Reddy T, Cournapeau D, Burovski E, Peterson P, Weckesser W, Bright J, van der Walt SJ, Brett M, Wilson J, Millman KJ, Mayorov N, Nelson ARJ, Jones E, Kern R, Larson E, Carey CJ, Polat İ, Feng Y, Moore EW, VanderPlas J, Laxalde D, Perktold J, Cimrman R, Henriksen I, Quintero EA, Harris CR, Archibald AM, Ribeiro AH, Pedregosa F, van Mulbregt P, SciPy 1.0 Contributors. 2020. SciPy 1.0: fundamental algorithms for scientific computing in Python. *Nature Methods* **17**:261–272 DOI 10.1038/s41592-019-0686-2.

Vogel N, Uthicke S. 2012. Calcification and photobiology in symbiont-bearing benthic foraminifera and responses to a high CO_2 environment. *Journal of Experimental Marine Biology and Ecology* **424–425(3)**:15–24 DOI 10.1016/j.jembe.2012.05.008.

Wang X, Wang M, Jia Z, Song X, Wang L, Song L. 2017. A shell-formation related carbonic anhydrase in *Crassostrea gigas* modulates intracellular calcium against CO_2 exposure: implication for impacts of ocean acidification on mollusk calcification. *Aquatic Toxicology* **189**:216–228 DOI 10.1016/j.aquatox.2017.06.009.

Wit JC, De Nooijer LJ, Barras C, Jorissen FJ, Reichart GJ. 2012. A reappraisal of the vital effect in cultured benthic foraminifer *Bulimina marginata* on Mg/Ca values: assessing temperature uncertainty relationships. *Biogeosciences* **9(9)**:3693–3704 DOI 10.5194/bg-9-3693-2012.

Zeebe RE, Wolf-Gladrow DA. 2001. *CO_2 in seawater: equilibrium, kinetics, isotopes*. Amsterdam: Elsevier.